

# Fast Azimuthal Displacement Retrieval from TOPSAR Burst Overlapping Interferometry: Application in Dronning Maud Land (Antarctica)

Quentin Glaude<sup>a,b</sup>, Dominique Derauw<sup>b,c</sup>, Christian Barbier<sup>b</sup>, and Frank Pattyn<sup>a</sup>

<sup>a</sup>Laboratoire de Glaciologie, Université Libre de Bruxelles, Bruxelles, Belgium

<sup>b</sup>Centre Spatial de Liège, Université de Liège, Angleur, Belgium

<sup>c</sup>Instituto de Investigación en Paleobiología y Geología, Universidad Nacional De Rio Negro, General Roca, Argentina

## Abstract

Differential SAR Interferometry allows deriving velocity maps only along the line of sight. Bi-dimensional displacement estimation may be overcome using TOPSAR mode acquisition. TOPSAR acquisition mode implies burst-by-burst acquisition with beam steering from backward to forward during burst acquisition. Consecutive bursts have a superposition area to allow proper stitching. In these superposition areas, each point is observed twice with different azimuthal viewing angles (i.e. backward and forward). Burst Overlapping Interferometry (BOI) exploits these superposition areas to extract azimuthal displacements. We present here results of the BOI technique applied on Antarctic ice shelves, i.e. fast-moving area, and propose a filtering algorithm.

## 1 Introduction

Synthetic Aperture Radar (SAR) gained increasing interest in the remote sensing community, due to day-and-night, and almost atmospheric-free characteristics of the Radar wavelength. This is particularly the case using differential SAR interferometry (DInSAR) to monitor ground displacements [1]. Sentinel-1, the SAR component of Copernicus, uses the TOPSAR acquisition mode [2] in order to reduce the revisit time and increase its coverage.

One major issue with DInSAR is the displacements being observed only in the line-of-sight of the sensor. In addition, it suffers from some limitations related to spaceborne SAR acquisition geometry. SAR Earth observation satellites use polar heliosynchronous orbits. Consequently, since sensors are acquiring data perpendicular to their orbits, differential interferometry allows getting principally the East-West displacement component of horizontal displacements, while displacements in the along-track direction stay unresolved. TOPSAR acquisition mode offers unique peculiarities to infer azimuthal displacements. In this mode, the sensor steers its beam from backward to forward, forming a burst, instead of looking perpendicular to the satellite track direction. This steering reduces the aperture synthesis acquisition time and allows to aim the beam at different parallel sub-swaths (and thus increases its coverage up to 400 kilometers). Finally, bursts are stitched together using overlapping bands as shown in Figure 1 and formed an observing scene.

In these overlapping areas, displacements occurring in the azimuth direction induce additional interferometric phase terms. By exploiting these overlapping areas, Burst Overlapping Interferometry (BOI) can retrieve the azimuthal

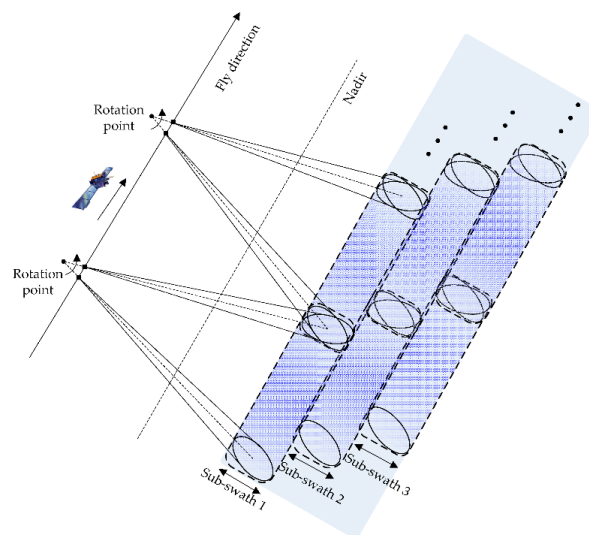


**Figure 1** Acquisition geometry of a TOPSAR image. The image is composed of sub-swaths and bursts with overlapping areas. Illustration from [3].

component of the displacement.

This technique has been recently used by several authors to produce at high accuracy along-track displacements [4, 5], and by using several passes, reconstruct three-dimensional displacement maps [6, 7, 8].

In this article, we present results obtained by applying the technique in a fast-moving context in Antarctica. Additionally, we propose a modified Goldstein filtering algorithm adapted to suit BOI geometric specificities.

## 2 Method

### 2.1 Burst Overlapping Interferometry

In TOPSAR superposition areas, ground scatterers are observed twice; firstly with the sensor behind the scattering element aiming forward, and once on the next burst, with the sensor in front of the scatterer, aiming backward. Since interferograms can be generated on a burst-by-burst basis, a backward and a forward interferogram can be generated on bursts superposition areas.

For classical DInSAR purposes, azimuthal displacements are biasing the interferometric signal by adding phase information. This phase component is equal in absolute value but opposite in sign in the backward and forward interferograms. Burst Overlapping Interferometry (BOI) consists of performing differential interferometry between backward and forward interferograms in the overlapping areas in order to cancel out all phase terms except the one induced by the azimuth component of local displacements (Figure 2).

The burst overlapping interferometric phase  $\phi_{BOI}$  is linearly proportional to an azimuthal displacement  $x$  (in pixel unit) by the relation :

$$\phi_{BOI} = \frac{2\pi \cdot \Delta f \cdot x}{AF} \quad (1)$$

where  $AF$  is the azimuthal frequency and  $\Delta f$  if the spectral separation. By inverting the equation, we obtain an azimuthal displacement :

$$x_{az} = \frac{AF}{2\pi \cdot \Delta f} \cdot \phi_{BOI} \quad (2)$$

This is the same relation as the one presented in extended spectral diversity techniques in order to remove small azimuth shifts in stationary areas.

### 2.2 Accuracy Estimation

The variance propagation results from the variance of individual interferograms [9], leading to the estimated displacement accuracy :

$$\sigma_x = \frac{AF}{2\pi \cdot \Delta f} \cdot \frac{1}{\sqrt{N}} \cdot \sqrt{\frac{1 - \gamma^2}{\gamma^2}} \quad (3)$$

where  $\gamma$  is the estimated coherence and  $N$  is the number of looks.

Using azimuth frequency of 342.46 Hz (Extended interferometric Wide-swath mode) and a median value of the Doppler frequency difference  $\Delta f$  of 5798 Hz/sec, we can simulate the accuracy in terms of standard deviation. This accuracy can be expressed in terms of pixel or phase value. Even for the case of fast displacement, the BOI phase is rather low varying in space. It allows us to increase the number of looks and reach the lower part of Table 1. Also, after filtering, the coherence can be quite high (see next section).

**Table 1** Estimation of the phase standard deviation (in degree) according to the coherence (columns) and the number of looks (rows).

	0.5	0.6	0.7	0.8	0.9
1	99.4	76.5	58.5	43.0	27.8
3	57.4	44.2	33.8	24.8	16.0
12	28.7	22.1	16.9	12.4	8.0
48	14.3	11.0	8.4	6.2	4.0

Note that the 4-degrees error present in the table (coherence of 0.9 and 48 looks) corresponds to a displacement of 1.2 cm between 2 acquisitions (i.e. 6 days). Said in other words, the estimated accuracy of azimuthal displacement from BOI can reach a displacement rate of 2mm/day (73cm/year). This is more than 10 times better than offset tracking results with Sentinel-1 [10].

### 2.3 BOI-Adapted Goldstein Phase Filtering

Phase computed using the BOI technique is quite noisy. Since the BOI phase is a difference between two phases, the noise component is increased by a  $\sqrt{2}$  factor. Moreover, the scatterer is observed from slightly different view angles, resulting in geometric decorrelation.

Goldstein phase filtering is a very popular phase filter algorithm [11]. The method is easy to implement, has few parameters and significantly filters results while preserving sharp spatial changes. These constitute the reasons why we built our BOI-adapted phase filtering based on the Goldstein phase filtering.

The elongated characteristic of the burst overlapping areas (around  $100 \times 8000$  pixels in EW mode) makes the Goldstein algorithm quite obsolete. We adapted the filter as a sliding window inside which an iterative low Goldstein phase filtering is employed. The filter produces the filtered BOI phase column by column when moving (Figure 4). No weighted average is implemented since the column by column sliding ensures a continuous estimation of the BOI phase.

## 3 Results

BOI has been applied on the Roi Baudouin Ice Shelf, in Queen Maud Land, Antarctica (Figure 5).

The application of BOI in Antarctica is tricky because of the fast-moving nature of the ice at the surface. This is particularly the case in the boundaries of Antarctica, at the surface of ice shelves.

The azimuthal displacement in BOI is expressed as a phase value. Here, we call azimuthal displacement ambiguity the azimuthal displacement leading to a 2-pi shift. Using equation (2), a 2-pi shift corresponds to a 0.059 pixel azimuthal displacement, this is to say a 1.176 meters displacement (pixel spacing of 19.9281 meters). When using SAR pairs with a 6-days revisit time, any displacement greater than 71.5 meters per year will wrap the BOI phase. On the Roi Baudouin Ice Shelf, displacements on the main ice stream

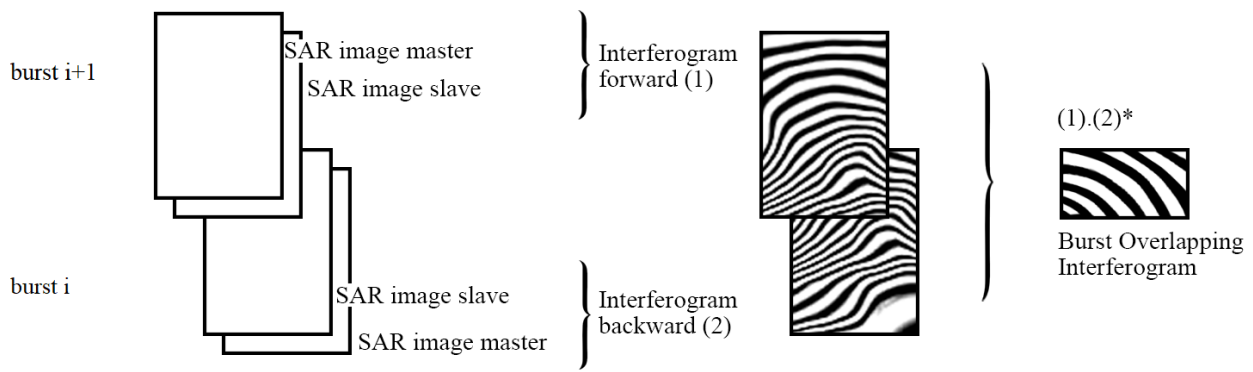


**Figure 2** Burst Overlapping Interferometry (BOI).

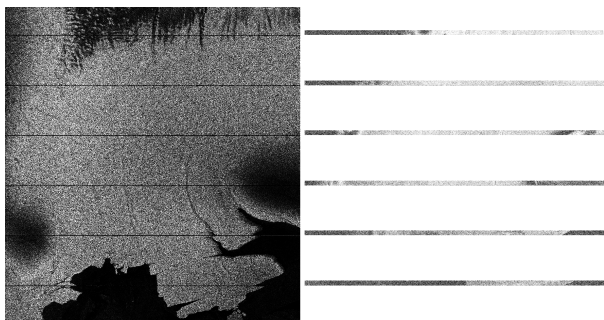


**Figure 3** The intensity of the master image (left) and BOI coherence (right). Coherence in our 1-look burst-overlap interferogram lies around 0.8 on the core of the shelf

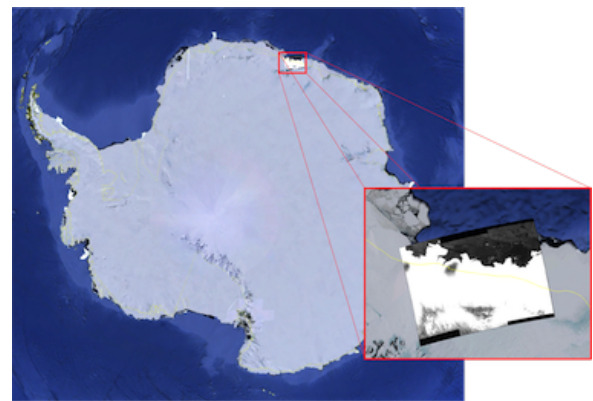


**Figure 5** Roi Baudouin Ice Shelf, Queen Maud land, Antarctica.

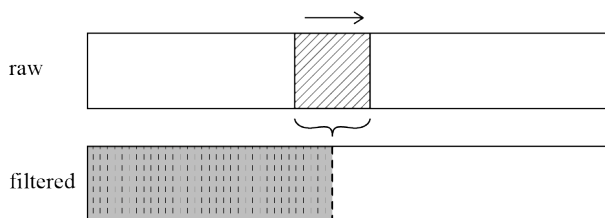


**Figure 4** Concept of the BOI-adapted Goldstein phase filtering. The Goldstein filter is applied iteratively as a moving window that generates the output phase column-by-column.

go further than 300 meters per year. Using references and unwrapping the signal allows obtaining the absolute azimuthal velocity. An example of the filter and the wrapped BOI signal is displayed in Figure 6.

## 4 Conclusion

DInSAR allows to derive at high accuracy displacements maps in the line-of-sight direction. With the specificities of Sentinel-1 and its particular acquisition TOPSAR mode, we can also use BOI in order to extract the azimuthal component of surface displacements.

In the present study, we applied the BOI technique in Antarctica. Considering the fast-moving nature of the observed surface, we showed that the BOI signal can be wrapped. Proper unwrapping is needed before conversion into azimuthal displacements. In addition, we proposed a Goldstein-adapted BOI phase filtering to filter the BOI phase.

Our results suggest that BOI and our developed filter are working properly. We can retrieve azimuthal displacement in fast-moving areas with a single SAR with centimeter accuracy.

## 5 Acknowledgment

This research is supported by the French Community of Belgium in the funding context of a FRIA grant, and carried out in the framework of the MIMO (Monitoring melt where Ice Meets Ocean) project funded by the Belgian Science Policy contract Nos. SR/00/336.

## 6 Literature

- [1] Massonnet, D.: Rossi, M.: Carmona, C.: Adragna, F.: Peltzer, G.: Feigl, K.: Rabaute, T.: The displacement

**Figure 6** Example of the application of our BOI-Adapted Goldstein phase filtering. Top: raw BOI Phase. Bottom: filtered phase. In the illustration, we focus on the BOI phase of the third burst overlapping area in figure 3.

- field of the Landers earthquake mapped by radar interferometry. *Nature*, 364(6433), 1993, pp. 138–142
- [2] De Zan, F.: Guarnieri, A. M.: TOPSAR: Terrain observation by progressive scans. *IEEE Transactions on Geoscience and Remote Sensing*, 44(9), 2006, pp. 2352–2360
- [3] Yang, W.: Chen, J.: Zeng, H.C.: Wang, P.B.: Liu, W.: A Wide-Swath Spaceborne TOPS SAR Image Formation Algorithm Based on Chirp Scaling and Chirp-Z Transform. *Sensors* 2016, 16, 2095
- [4] Jiang, H. J.: Pei, Y. Y.: Li, J.: Sentinel-1 TOPS interferometry for along-track displacement measurement, *IOP Conf. Ser.: Earth Environ. Sci.* 57 012019, 2017
- [5] Mancon, S.: Monti Guarnieri, A.: Giudici, D.: Tebaldini, S.: On the Phase Calibration by Multisquint Analysis in TOPSAR and Stripmap Interferometry, in *IEEE Transactions on Geoscience and Remote Sensing*, vol. 55, no. 1, pp. 134–147, Jan. 2017.
- [6] Jiang, H.: Feng, G.: Wang, T.: Bürgmann, R.: Toward full exploitation of coherent and incoherent information in Sentinel-1 TOPS data for retrieving surface displacement: Application to the 2016 Kumamoto (Japan) earthquake, *Geophys. Res. Lett.*, 44, 2017, pp. 1758–1767
- [7] Grandin, R.: Klein, E.: Métois, M.: Vigny, C.: Three-dimensional displacement field of the 2015 Mw8.3 Illapel earthquake (Chile) from across- and along-track Sentinel-1 TOPS interferometry, *Geophys. Res. Lett.*, 43, 2016, pp. 2552–2561
- [8] Prats-Iraola, P.: Member, S.: Lopez-dekker, P.: Member, S.: De Zan, F.: Yagüe-Martínez, N.: Rodríguez-cassola, M.: Performance of 3-D Surface Deformation Estimation for Simultaneous Squinted SAR Acquisitions, 56(4), 2018, pp. 2147–2158.
- [9] Just, D.: Bamler, R.: Phase statistics of interferograms with applications to synthetic aperture radar, *Appl. Opt.* 33, 4361–4368, 1994
- [10] Mouginot, J.: Rignot, E.: Scheuchl, B.: & Millan, R.: Comprehensive annual ice sheet velocity mapping using Landsat-8, Sentinel-1, and RADARSAT-2 data. *Remote Sensing*, 9(4), 2017, pp. 1–20
- [11] Goldstein, R.: Werner, C.: Radar interferogram filtering for geophysical applications. *Geophysical Research Letters*, 25, 1998, pp. 4035–4038